J. Phys. B: At. Mol. Opt. Phys. **24** (1991) 2589–2599. Printed in the UK

Determination of the electron–ion dissociative recombination coefficients for several molecular ions at 300 K

Mark Geoghegan†, Nigel G Adams‡ and David Smith

School of Physics and Space Research, University of Birmingham, Birmingham B15 2TT, UK

Received 9 November 1990, in final form 28 February 1991

Abstract. The electron–ion dissociative recombination rate coefficients, α_e, have been determined for ten molecular ions, seven of which have not previously been measured. The data were obtained under truly thermal conditions at 300 K using a flowing afterglow/Langmuir probe (FALP) apparatus. Recombination coefficients were obtained for the following ions: CO_2^+ ($\alpha_e = 3.1 \times 10^{-7}$ cm^3 s^{-1}), N_2^+ (2.0), CO^+ (1.6), KrH^+ (<0.2), XeH^+ (<0.4), HSO_2^+ (2.7), CH_3CNH^+ (3.3), CH_3CHOH^+ (3.9), $C_2H_5CNH^+$ (4.7) and $((CH_3)_2CO)_2H^+$ (14). The dissociative recombination of many of the ions studied may be important in planetary, cometary and terrestrial atmospheres and be involved in the synthesis of interstellar molecules.

1. Introduction

The rate coefficients, α_e, for dissociative recombination reactions are necessary for determining the ionization loss in many natural plasmas including the Earth's ionosphere and interstellar gas clouds (see, for example, the reviews by Smith and Adams 1980, 1989) and also in laboratory plasmas such as those in gas lasers (Biondi 1976) and in the etchant plasmas used in the creation of silicon chips (Turban 1984). A number of techniques have been used to determine α_e, including the stationary (microwave) afterglow technique (Frommhold *et al* 1968, Weller and Biondi 1968), the trapped ion technique (DuBois *et al* 1978), the merged electron–ion beam experiment (MEIBE) (Auerbach *et al* 1977) and the flowing afterglow/Langmuir probe (FALP) technique (Alge *et al* 1983). Rate coefficients are determined using the ion trap and the MEIBE by integrating cross section data over a Maxwell–Boltzmann distribution. The present study is an extension of previous work using the FALP technique to determine rate coefficients for the dissociative recombination of ground vibronic state diatomic and polyatomic ions (Alge *et al* 1983, Adams *et al* 1984, Adams and Smith 1988).

2. Experiment

The FALP technique has been described in detail previously (Alge *et al* 1983). Briefly, a microwave discharge is created upsteam in flowing helium carrier gas at a pressure

† Present address: Cavendish Laboratory, University of Cambridge, Cambridge CB3 0HE, UK.
‡ Present address: Department of Chemistry, University of Georgia, Athens, GA 30602, USA.

0953-4075/91/102589+11$03.50

of ~1.2 Torr. The afterglow consists of metastable helium atoms He^m and He^+ and He_2^+ ions. The He_2^+ ions are formed by collisions of metastable helium atoms in the discharge (the Hornbeck-Molnar process: Hornbeck and Molnar 1951) and in the three-body association of He^+ ions with helium atoms. Argon is often added to reactively remove metastable helium atoms and He_2^+ ions, forming Ar^+ in both cases. Thermal equilibrium is then rapidly achieved in collisions of ions and electrons with the helium carrier gas (Smith *et al* 1975).

The addition of sufficient hydrogen further downstream results in the formation of an H_3^+/electron plasma. H_2 reacts with the Ar^+ ions to form ArH^+ and some H_2^+ which both, in turn, react further with H_2 to form H_3^+. Since H_3^+ recombines only slowly (Adams *et al* 1984), the dominant ionization loss process in this H_3^+/electron plasma is by the comparatively slow process of ambipolar diffusion to the flow tube walls. By adding a reactant gas, X, further downstream, the ion under study, XH^+, is rapidly created by proton transfer from H_3^+ to X. This is a consequence of the relatively small proton affinity of H_2. Thus a wide variety of protonated ions, XH^+, can be created. This technique has been exploited previously using the FALP (Adams *et al* 1984, Adams and Smith 1988).

For the study of non-protonated ions, the ion X^+ may often be created simply by introducing the parent gas, X, into a plasma containing Ar^+ and He^+ ions. For example, after addition of CO_2 to an Ar^+/He^+ plasma, the following reaction sequence ensues:

$$He^+ \xrightarrow{CO_2} CO^+, CO_2^+ \tag{1}$$

$$CO^+ \xrightarrow{CO_2} CO_2^+ \tag{2}$$

$$Ar^+ \xrightarrow{CO_2} CO_2^+ \tag{3}$$

There is also a 9% O^+ product in the reaction of He^+ with CO_2 (Adams and Smith 1976) which reacts further with the CO_2 to form O_2^+. This may be neglected since when the CO_2^+ formed in reaction (3) is taken into account, less than 4% of the ions in the plasma are O_2^+. It is not always possible, however, to neglect minority ions. Addition of N_2 (or CO) to a helium afterglow will result in the formation of a plasma with N_2^+ (or CO^+) as the dominant ionic species but there will also be a significant amount of N^+ (or C^+) ions present which must be accounted for in any determination of α_e since they do not recombine or react further.

The movable Langmuir probe enables the measurement of electron number densities, n_e, at various points along the axis of the flow tube. A downstream quadrupole mass spectrometer is routinely used to monitor the ions present in the plasma.

When only one ion species is present in the plasma, determination of α_e is straightforward. In most cases, diffusion can be neglected compared with recombination and thus the reduction in electron density with distance is given by

$$v_p \frac{\partial n_e(z)}{\partial z} = -\alpha_e n_+(z) n_e(z) \tag{4}$$

where $n_+(z)$ and $n_e(z)$ are the positive ion and electron number densities respectively at a position z. v_p is the plasma flow velocity, determined as described by Adams *et al* (1975). Since the flowing afterglow is a true plasma then $n_+(z) = n_e(z)$ and the

solution to equation (4) is

$$\frac{1}{n_e(z)} = \frac{1}{n_e(0)} + \frac{\alpha_e z}{v_p} \tag{5}$$

Thus a plot of $1/n_e$ against z should be linear, allowing the determination of α_e from the gradient. All of the α_e reported in this paper (see table 1) were measured at a temperature of 300 K.

3. Results

3.1. CO_2^+

Addition of enough CO_2 to a plasma containing He^+ and Ar^+ ions ensures that a CO_2^+/electron plasma (neglecting the <4% O_2^+ ions present from the reaction of O^+ with CO_2) is created. The only loss processes for the CO_2^+ ions are dissociative recombination with a minor contribution due to ambipolar diffusion to the flow tube walls. A value of $\alpha_e(CO_2^+) = 3.1 \times 10^{-7}$ cm^3 s^{-1} was obtained from the gradient of the linear region of the $1/n_e$–z plot (see figure 1) using equation (5). Previous measurements of $\alpha_e(CO_2^+)$ are nearly 30% greater than this result, which is considered accurate to within 20%. These measurements, by Weller and Biondi (1967) and Gutcheck and Zipf (1973) yield rate coefficients of 3.8 and 4.0×10^{-7} cm^3 s^{-1} respectively at 300 K. Gutcheck and Zipf argue that there may have been a significant amount of vibrationally excited CO_2^+ in both of these experiments (they observed $CO(A\,^1\Pi(v'=3))$ emission from the dissociative recombination of CO_2^+, which is not energetically possible for ground vibronic state CO_2^+). However, Vallée *et al* (1986) point out that analysis of these experimental situations shows that vibrationally excited CO_2^+ would be quenched in near resonant charge exchange reactions with CO_2 before recombination could occur. In this respect, CO_2^+ in our experiment would be rapidly quenched and we therefore

Table 1. Rate coefficients, α_e, at 300 K for the recombination with electrons of the ions indicated. All of the above rate coefficients are subject to the systematic error in the area of the Langmuir probe (considered accurate to ±10% after allowing for end effects) and the plasma velocity (considered accurate to ±10%). These reflect directly in the measured rate coefficient. Relative rate coefficients have an uncertainty of ~10% less than absolute values.

Ion	$\alpha_e(10^{-7}$ cm^3 s$^{-1})$	Uncertainty
CO_2^+	3.1	20%
N_2^+	2.0	20%
CO^+	1.6	20%
KrH^+	<0.2	25%
XeH^+	<0.4	25%
HSO_2^+	2.7	20%
CH_3CNH^+	3.3	30%
CH_3CHOH^+	3.9	30%
$C_2H_5CNH^+$	4.7	40%
$((CH_3)_2CO)_2H^+$	14	40%

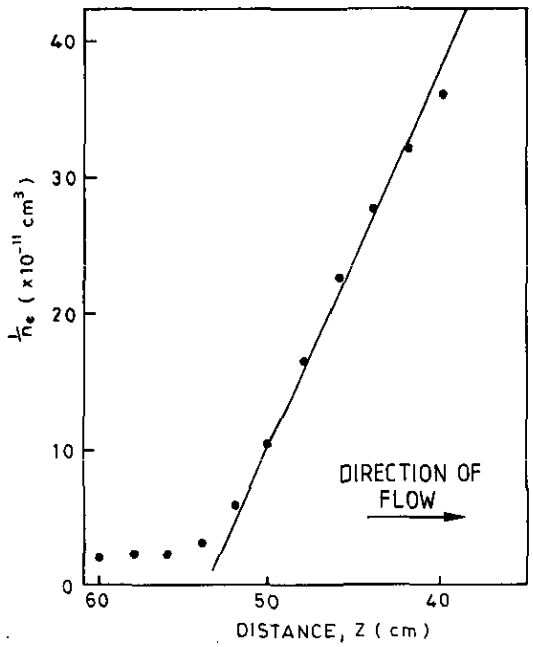

Figure 1. Plot of $1/n_e$ against distance, z, from the mass spectrometer sampling orifice for a CO_2^+ plasma. The CO_2 was introduced into the flow at an inlet 57.5 cm from the sampling orifice. $\alpha_e(CO_2^+) = 3.1 \times 10^{-7}$ cm^3 s^{-1} was obtained from the gradient of the linear region of this plot.

are confident that our measured rate coefficient of 3.1×10^{-7} cm^3 s^{-1} is that for the dissociative recombination of ground vibronic state CO_2^+.

3.2. N_2^+ and CO^+

As has been mentioned in section 2, the addition of N_2 or CO to the helium afterglow results in a plasma in which the dominant ion is N_2^+ or CO^+ respectively. However, in each case the remaining He^+ ions react with the parent gas to produce the atomic ions N^+ and C^+ (Fehsenfeld *et al* 1966, Adams and Smith 1976) which do not react further. Since these species do not recombine, the atomic ion number density decays only slowly by ambipolar diffusion to the flow tube walls. The N_2 and CO were introduced into the flow via the most downstream inlet, by which point the maximum possible amount of He^+ had associated with He to form He_2^+. The N_2 and CO number densities in the plasma were 1×10^{14} cm^{-3} and 4×10^{13} cm^{-3} respectively. This resulted in the rapid production of N_2^+ and CO^+ (as well as N^+ and C^+) but not of the cluster ions (confirmed by the use of the downstream mass spectrometer). Indeed, using the rate coefficient of 1.4×10^{-28} cm^6 s^{-1} at 300 K obtained by Meot-Ner and Field (1974) for the three-body association of CO^+ with CO (helium is the third body), an e-folding distance of 41 cm was calculated, larger than the length scale of the $1/n_e$-z plot. Similarly, using a rate coefficient of 1.8×10^{-29} cm^6 s^{-1} at 300 K for the three-body association of N_2^+ with N_2 in helium (Böhringer *et al* 1983) an even longer e-folding distance of 150 cm was obtained.

In order to analyse this situation the continuity equation for loss of N^+ ions, initially a fraction f of the total ion number density, by fundamental mode ambipolar diffusion

was first considered. This is given by;

$$\frac{\partial[N^+]_z}{\partial z} = -\frac{f n_0 D_a}{\Lambda^2 v_p} \exp(-D_a z/\Lambda^2 v_p) \tag{6}$$

where $[N^+]_z$ is the N^+ number density at distance z, n_0 is the initial electron number density, D_a, the ambipolar diffusion coefficient and Λ, the characteristic radial diffusion length of the flow tube. The loss of N^+ (and similarly C^+) along the axis of the flow tube can thus be determined.

The decay of electron number density $(=[N^+]_z+[N_2^+]_z)$ along the axis of the flow tube is given by

$$\frac{\partial n_e(z)}{\partial z} = -\frac{n_0 D_a}{\Lambda^2 v_p} \exp(-D_a z/\Lambda^2 v_p) - \alpha_e(n_e(z) - [N^+]_z)\frac{n_e(z)}{v_p} \tag{7}$$

where α_e is the dissociative recombination rate coefficient for N_2^+. Having determined $[N^+]_z$ by solution of equation (6), $n_e(z)$ can be obtained by using a simple iterative procedure on a microcomputer to numerically solve equation (7). In this analysis the same value of D_a was used for N_2^+ as for N^+ as there is only a ~10% difference between them (as is evident from the paper by Lindinger and Albritton (1975)). Figure 2 shows a $1/n_e$–z plot for a plasma containing N_2^+ and N^+ ions. The full curve was fitted to the data points by optimizing α_e, D_a and f. The best fit was for $\alpha_e(N_2^+) = 2.0\times10^{-7}\,cm^3\,s^{-1}$. Similarly, for $\alpha_e(CO^+)$, a value of $1.6\times10^{-7}\,cm^3\,s^{-1}$ was obtained; the fit to the data is shown in figure 2. A value of D_a of $600\,cm^2\,s^{-1}$ was obtained in both cases although $700\,cm^2\,s^{-1}$ may be considered more appropriate from the literature. In any event, the D_a in the computer fits have little effect on the best values of α_e as ambipolar diffusion is negligible compared to dissociative recombination in the upstream region of the plot. Also values of f of 0.32 and 0.30 were obtained in the determination of $\alpha_e(N_2^+)$ and $\alpha_e(CO^+)$ respectively. These values are reasonable since N_2^+ and CO^+ are predominantly produced in the reaction of N_2 and CO with He^m.

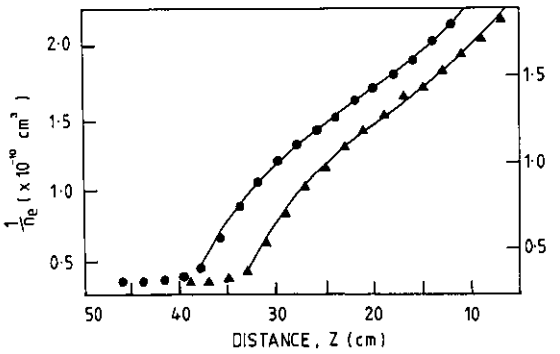

Figure 2. Plots of $1/n_e$ against distance, z for plasmas containing N_2^+ and N^+ ions (●) and CO^+ and C^+ ions (▲). N_2 and CO were added at the downstream inlet ($z = 39$ cm). The computer fits (full curves) give $\alpha_e(N_2^+) = 2.0\times10^{-7}\,cm^3\,s^{-1}$ and $\alpha_e(CO^+) = 1.6\times10^{-7}\,cm^3\,s^{-1}$. Note the decreasing gradient with distance downstream as the N^+ (or C^+) becomes more significant as the N_2^+ (or CO^+) recombines away with electrons. Further downsteam the gradient starts to increase again due to the increasing contribution of ambipolar diffusion to the ionization loss process. Note that the plot for the plasma containing CO^+ and C^+ ions has been shifted by subtracting 5 cm from z for clarity and that the right-hand ordinates correspond to $1/n_e$ for this plasma.

However, since there is a 100% C^+ product channel in the $He^+ + CO$ reaction but only a 60% N^+ channel in the $He^+ + N_2$ reaction (Adams and Smith 1976), one might expect the value of f for N^+ to be less than that for C^+. In our experiment, N_2^+ formation was over twice as rapid as that for CO^+. Recombination of N_2^+ upstream of the point where n_0 was determined is responsible for the larger value of f in the determination of $\alpha_e(N_2^+)$.

The dissociative recombination rate coefficient for N_2^+ is presently the subject of some doubt. Mehr and Biondi (1969) obtained a value of 1.8×10^{-7} cm^3 s^{-1} using the stationary afterglow technique with neon buffer gas. Zipf (1980) obtained 2.2×10^{-7} cm^3 s^{-1} using laser induced photofluorescence to observe the vibrational states of N_2^+ in his stationary afterglow. Zipf concluded that $\alpha_e(N_2^+)$ does not vary significantly with vibrational excitation (for low v). Noren *et al* (1989) claim that $\alpha_e(N_2^+(v=0))$ is a factor of ~5 less than these values, and they observe a significant enhancement in α_e with increasing vibrational excitation. In their experiment, using the merged beam apparatus, the vibrational state of N_2^+ is selected by examining the threshold for electron impact excitation of the ion. Noren *et al* argue that afterglow experiments necessitate use of a minimal amount of N_2 in order to inhibit three-body reactions of N_2^+. They further argue that the small amount of N_2 present cannot prevent significant re-excitation of N_2^+ ions in the reverse direction of the rapid resonant charge exchange reaction

$$N_2^+(v>0) + N_2(v=0) \rightleftharpoons N_2(v>0) + N_2^+(v=0) \tag{8}$$

This cannot be the case in our experiment (or indeed, those of Mehr and Biondi (1969) and Zipf (1980)) since the N_2 number density is some 10^4 times greater than that of N_2^+. Thus the forward direction of (8) will be completely dominant, and re-excitation negligible. Lindinger *et al* (1981) estimated a value of 4×10^{-10} cm^3 s^{-1} for the quenching of N_2^+ by N_2 using a drift tube (although the N_2^+ vibrational distribution will be different to that in our plasma). This would ensure sufficiently rapid quenching of $N_2^+(v>0)$.

N_2^+ is a particularly important ion in the Earth's atmosphere since its dissociative recombination, along with that of NO^+ and O_2^+, is almost entirely responsible for the ionization loss in the *E*-region of the atmosphere. Modellers of the chemistry of the atmosphere would obviously desire a universally accepted value of $\alpha_e(N_2^+)$. We have defended the use of afterglows in determining $\alpha_e(N_2^+)$ but present no explanation for the discrepancy between afterglow and merged beam results.

The result of 1.6×10^{-7} cm^3 s^{-1} for $\alpha_e(CO^+)$ is also somewhat greater than that of 1.0×10^{-7} cm^3 s^{-1}, obtained using the MEIBE† (Mitchell and Hus 1985). This difference is however less serious. An earlier result of $\alpha_e(CO^+)$ of 6.8×10^{-7} cm^3 s^{-1} (Mentzoni and Donohue 1969) can be dismissed as being too large due to cluster formation in their carbon monoxide afterglow. The dissociative recombination of CO^+ is thought to be important in cometary atmospheres (Huebner 1985).

3.3. *KrH^+ and XeH^+*

The creation of these ions was by proton transfer from H_3^+ to the parent neutral. Since Kr has a proton affinity of only 0.7 kcal mol^{-1} greater than H_2 (Bohme *et al* 1980), care was taken to limit the amount of H_2 in the flow tube to inhibit the reverse reaction

† A calibration error in the MEIBE has meant that the α_e values published between 1977 and 1985 have to be reduced by a factor of two. The papers quoted are those which report the experiment, but the rate coefficients have been taken from the list in the review by Mitchell (1990).

(although enough was used to ensure that H_3^+ was rapidly formed). The Kr number density in the flow tube was over four times greater than that for H_2 and the e-folding distance for the forward reaction;

$$H_3^+ + Kr \rightleftharpoons KrH^+ + H_2 \tag{9}$$

was less than 0.4 cm and that for the reverse reaction, over 40 cm (using rate coefficients determined by Bohme *et al* 1980). To the authors' knowledge, the rate coefficient for the proton transfer reaction of H_3^+ with Xe had not been measured. In a parallel selected ion flow tube (SIFT) study at 300 K this was determined to be 2.4 ($\pm$0.6) $\times$ 10^{-9} cm^3 s^{-1}.

Neither of the two ions, KrH^+ nor XeH^+, were observed to recombine at a significant rate. Upper limits of 2 and 4×10^{-8} cm^3 s^{-1} were obtained for the respective recombination rate coefficients. These upper limits are uncertain to $\pm$25% because of the small range of n_e from which α_e was determined. The plots of ln n_e against z, shown in figure 3, are both linear, indicating that ambipolar diffusion was the major ionization loss process. From these plots reduced mobilities, μ_0, of $\sim$14 and $\sim$21 cm^2 V^{-1} s^{-1} were determined for KrH^+ and XeH^+ respectively. The rather large value of $\mu_0(XeH^+)$ would appear to indicate that a small amount of dissociative recombination of XeH^+ was occurring in the plasma. Unfortunately, there are no literature values of $\mu_0(XeH^+)$ in helium to compare with that obtained in our study but one might expect $\mu_0(XeH^+)$ to be similar to the value of 18 cm^2 V^{-1} s^{-1} determined for Xe^+ in helium (Chen 1963).

The dissociative recombination rate coefficients of few protonated atoms have so far been determined. As well as the above, α_e has been determined for H_2^+ (Hus *et al* 1988), HeH^+ (Adams and Smith 1989, Yousif and Mitchell 1989), CH^+ (Mitchell and McGowan 1978), OH^+ (Mul *et al* 1983) and NH^+ (McGowan *et al* 1979). Of these, only CH^+ has been observed to recombine rapidly, with a rate coefficient† of 1.5×10^{-7} cm^3 s^{-1}; the other ions have $\alpha_e < 5 \times 10^{-8}$ cm^3 s^{-1}. However, the vibrational distribution of the recombining CH^+ was undetermined. Mitchell (1990) has indicated that a study of the dissociative recombination of vibrationally cold CH^+ will be undertaken.

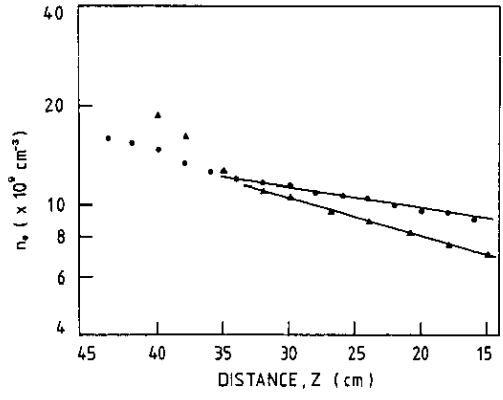

Figure 3. Logarithmic plots of n_e against distance, z for plasmas containing KrH^+ (●) and XeH^+ (▲). The linearity of these plots indicates that dissociative recombination is not the major ionization loss process. Reduced mobilities of $\sim$14 and $\sim$21 cm^2 V^{-1} s^{-1} for KrH^+ and XeH^+ respectively were determined from the gradient of these plots. These must, however be considered upper limits (see text). The reactant gases (Kr and Xe) were introduced into the flow at $z = 39$ cm. Note that $\sim$5 cm is required to produce the required plasma and to allow it to relax into a fundamental mode diffusion profile.

In the absence of experimental data, it is often assumed that diatomic ions recombine rapidly with $\alpha_e > 10^{-7}$ cm^3 s^{-1} at 300 K (see, for example, the compilation by Prasad and Huntress (1980)). The limited data available indicate that this may not be the case for protonated atoms.

3.4. HSO_2^+, CH_3CNH^+, CH_3CHOH^+, $C_2H_5CNH^+$ and $(CH_3)_2COH^+$

The above ions were created by proton transfer from H_3^+ to the parent gas or vapour. The rate coefficients for these proton transfer reactions are large and have all been measured previously (Rakshit 1982, Giles 1990, Herbst *et al* 1990) except for the $H_3^+ + C_2H_5CN$ reaction. The rate coefficient for this reaction was determined to be 9.6 $(\pm 3.4) \times 10^{-9}$ cm^3 s^{-1} at 300 K in a parallel SIFT study.

The study of the dissociative recombination of HSO_2^+ was significantly more straightforward than for the other four ions in this section since clustering was not observed to occur. A value of 2.7×10^{-7} cm^3 s^{-1} was obtained for $\alpha_e(HSO_2^+)$. Figure 4 shows the $1/n_e$–z plot for a recombining HSO_2^+/electron plasma.

In order to determine α_e for CH_3CNH^+ and CH_3CHOH^+, the parent vapour number density had to be kept small in order to inhibit the formation of clustered species. This also meant that the formation of XH^+ extended over a somewhat greater distance in the flow tube (the e-folding distance is 2 cm for both CH_3CNH^+ and CH_3CHOH^+ production). As a result significant dissociative recombination of XH^+ occurred in the region of the flow tube where the XH^+ plasma was being formed, reducing the range of n_e that the $1/n_e$–z plot is linear over (see figure 4). Thus an uncertainty of ±30% in α_e is considered appropriate for these two ions.

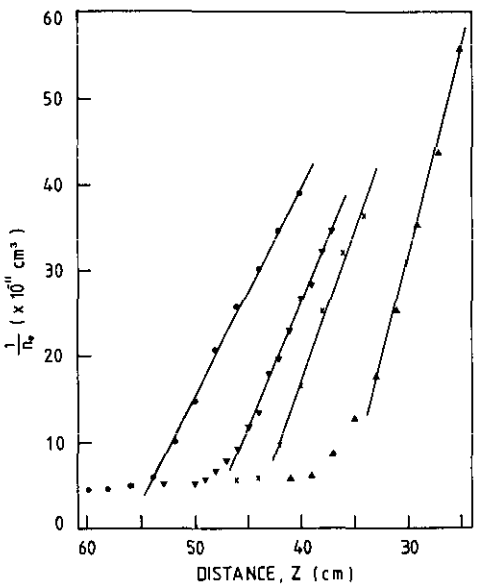

Figure 4. Plots of $1/n_e$ against distance, z for recombining HSO_2^+ (●), CH_3CNH^+ (▼), CH_3CHOH^+ (×) and $C_2H_5CNH^+$ (▲) plasmas. Recombination coefficients of 2.7, 3.3, 3.9 and 4.7×10^{-7} cm^3 s^{-1} were determined for the respective ions from the gradient of the linear region of each plot. The parent gas or vapour was introduced at the inlet 57.5 cm from the mass spectrometer sampling orifice. For clarity, the latter three plots have each been staggered by subtracting 5, 10 and 15 cm respectively from z.

A complicating factor in the determination of α_e for $C_2H_5CNH^+$ and $(CH_3)_2COH^+$ is that proton transfer from H_3^+ to the parent vapour is partly dissociative:

$$H_3^+ + C_2H_5CN \rightarrow H_2CN^+ + C_2H_4 + H_2 \quad 0.65 \quad (10a)$$

$$\rightarrow C_2H_5CNH^+ + H_2 \quad 0.25 \quad (10b)$$

$$\rightarrow C_2H_5^+ + HCN + H_2 \quad 0.10 \quad (10c)$$

$$H_3^+ + (CH_3)_2CO \rightarrow (CH_3)_2COH^+ + H_2 \quad 0.50 \quad (11a)$$

$$\rightarrow H_3CO^+ + C_2H_4 + H_2 \quad 0.35 \quad (11b)$$

$$\rightarrow C_3H_5^+ + H_2O + H_2 \quad 0.10 \quad (11c)$$

$$\rightarrow CH_3CO^+ + CH_4 + H_2 \quad 0.05. \quad (11d)$$

The products for reaction (10) were determined in a parallel SIFT study and those for reaction (11) are taken from the paper by Herbst *et al* (1990). The product distributions are considered accurate to within ±0.05. Secondary reactions of the product ions with the parent vapour ensured that the ion under study was rapidly created. Indeed, when determining $\alpha_e(C_2H_5CNH^+)$, only $C_2H_5CNH^+$ and its first cluster ion were observed at the downstream mass spectrometer. The observation of cluster ions in the mass spectrum does not necessarily imply that the cluster ion is contributing significantly to the recombination; at the mass spectrometer sampling orifice, n_e is often so small that clustering dominates over recombination. Since a small C_2H_5CN number density is necessary to inhibit cluster formation, and because of the dissociative proton transfer from H_3^+ to C_2H_5CN, a ±40% uncertainty is appropriate for $\alpha_e(C_2H_5CNH^+)$. The $1/n_e$–z plot used in determining $\alpha_e(C_2H_5CNH^+)$ is included in figure 4.

In the case of the study of protonated acetone, $(CH_3)_2COH^+$, the clustered species $CH_3CO^+(CH_3)_2CO$ was observed in the mass spectrum as well as the expected ions $(CH_3)_2COH^+$ and $((CH_3)_2CO)_2H^+$. The existence of $CH_3CO^+(CH_3)_2CO$ in the mass spectrum is attributed to the fact that proton transfer from CH_3CO^+ to acetone is endothermic. Thus the ion under study, $(CH_3)_2COH^+$ was not created from the secondary reaction of CH_3CO^+ which instead associated with acetone. Fortunately however, CH_3CO^+ is only a 5% product of reaction (11) and so the presence of $CH_3CO^+(CH_3)_2CO$ in the plasma can be neglected. Since clustering was dominant, we did not succeed in measuring $\alpha_e((CH_3)_2COH^+)$ but it was possible to measure α_e for $((CH_3)_2CO)_2H^+$. In this case a ±40% uncertainty is appropriate due to the possible contribution of the dissociative recombination of higher order clusters (see figure 5).

The dissociative recombination of these ions, with the exception of $((CH_3)_2CO)_2H^+$, may be involved in the synthesis of interstellar molecules since SO_2, CH_3CN, C_2H_5CN, CH_3CHO (and $(CH_3)_2CO$) have all been detected in interstellar gas clouds (see, for example, the reviews by Turner (1989) and Smith and Adams (1989) for full lists of observed interstellar molecules). These results will therefore be useful to astrochemists for use in models of molecular synthesis in dense interstellar clouds. Note that the determination of the rate coefficients for the dissociative recombination of these protonated molecules at temperatures approaching those of interstellar clouds (~10 K) is not possible using the FALP (this apparatus can be operated at temperatures down to 90 K) since the parent gas or vapour would condense on the flow tube walls and inlet pipes.

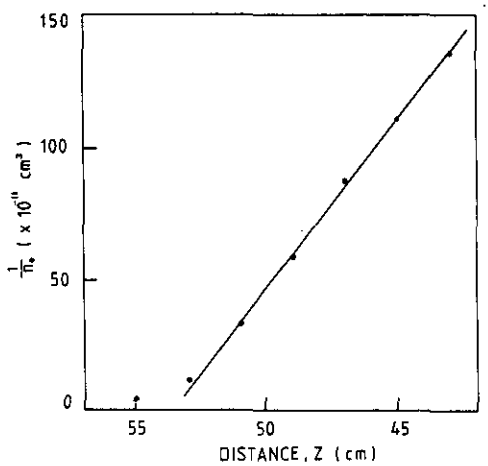

Figure 5. Plot of $1/n_e$ against distance, z for a plasma containing mainly $((CH_3)_2CO)_2H^+$ ions. A rate coefficient of 1.4×10^{-6} cm^3 s^{-1} was determined for $\alpha_e(((CH_3)_2CO)_2H^+)$ from the gradient of this plot. Since the plot is linear over an order of magnitude decrease in n_e, it would appear that higher order clusters do not have significantly different recombination coefficients.

4. Summary

Dissociative recombination rate coefficients have been determined for ten ground vibronic state molecular ions. Values of α_e vary from 1.4×10^{-6} cm^3 s^{-1} for the cluster ion $((CH_3)_2CO)_2H^+$ down to an upper limit of 2×10^{-8} cm^3 s^{-1} for $\alpha_e(KrH^+)$; a variation of at least two orders of magnitude. A general increase in α_e with ion complexity, as discussed by Biondi (1973) is observed here. Bates (1991) has very recently considered theoretically the recombination of cluster ions. He concludes that, for cluster ions of species with large proton affinities, there is insufficient energy for electronic excitation of the products and that, as a consequence, a fast single electron, radiationless transition occurs. Large recombination coefficients would therefore be expected. Seven of the rate coefficients presented in this paper have not previously been measured to our knowledge and they will thus add to the body of data already available (see the review by Mitchell 1990).

Acknowledgments

We would like to acknowledge Drs Kevin Giles and Christopher A Mayhew for their help in obtaining the experimental data. We are grateful to Mr Neville Buttress for preparing the diagrams. This work was funded by the United States Air Force, to whom MG is also extremely grateful for a research studentship.

References

Adams N G, Church M J and Smith D 1975 *J. Phys. D: Appl. Phys.* **8** 1409-22
Adams N G and Smith D 1976 *J. Phys. B: At. Mol. Phys.* **9** 1439-51
—— 1988 *Chem. Phys. Lett.* **144** 11-14

Adams N G and Smith D 1989 *Dissociative Recombination: Theory, Experiment and Applications* ed J B A Mitchell and S L Guberman (Singapore: World Scientific) pp 124–40
Adams N G, Smith D and Alge E 1984 *J. Chem. Phys.* **81** 1778–84
Alge E, Adams N G and Smith D 1983 *J. Phys. B: At. Mol. Phys.* **16** 1433–44
Auerbach D, Cacak R, Caudano R, Gaily T D, Keyser C J, McGowan J Wm, Mitchell J B A and Wilk S F J 1977 *J. Phys. B: At. Mol. Phys.* **10** 3797–819
Bates D R 1991 *J. Phys. B: At. Mol. Opt. Phys.* **24** 703–9
Biondi M A 1973 *Comment. At. Mol. Phys.* **4** 85–91
—— 1976 *Principles of Laser Plasmas* ed G Bekefi (New York: Wiley-Interscience) pp 125–57
Bohme D K, Mackay G I and Schiff H I 1980 *J. Chem. Phys.* **73** 4976–86
Böhringer H, Arnold F, Smith D and Adams N G 1983 *Int. J. Mass Spectrom. Ion Phys.* **52** 25–41
Chen C L 1963 *Phys. Rev.* **131** 2550–5
DuBois R D, Jeffries J B and Dunn G H 1978 *Phys. Rev.* A **17** 1314–20
Fehsenfeld F C, Schmeltekopf A L, Goldan P D, Schiff H I and Ferguson E E 1966 *J. Chem. Phys.* **44** 4087–94
Frommhold L, Biondi M A and Mehr F J 1968 *Phys. Rev.* **165** 44–52
Giles K 1990 *PhD Thesis* (Birmingham: University of Birmingham)
Gutcheck R A and Zipf E C 1973 *J. Geophys. Res.* **78** 5429–36
Herbst E, Giles K and Smith D 1990 *Astrophys. J.* **358** 468–72
Hornbeck J A and Molnar J P 1951 *Phys. Rev.* **84** 621–5
Huebner W F 1985 *The Photochemistry of Atmospheres* ed J S Levine (Orlando, FL: Academic) pp 437–81
Hus H, Yousif F B, Noren C, Sen A and Mitchell J B A 1988 *Phys. Rev. Lett.* **60** 1006–9
Lindinger W and Albritton D L 1975 *J. Chem. Phys.* **62** 3517–22
Lindinger W, Howorka F, Lukac P, Kuhn S, Villinger H, Alge E and Ramler H 1981 *Phys. Rev.* A **23** 2319–26
McGowan J Wm, Mul P M, D'Angelo V S, Mitchell J B A, Defrance P and Froelich H R 1979 *Phys. Rev. Lett.* **42** 373–5
Mehr F J and Biondi M A 1969 *Phys. Rev.* **181** 264–71
Mentzoni M H and Donohue J 1969 *Phys. Lett.* A **26** 330–1
Meot-Ner M and Field F H 1974 *J. Chem. Phys.* **61** 3742–9
Mitchell J B A 1990 *Phys. Rep.* **186** 215–48
Mitchell J B A and Hus H 1985 *J. Phys. B: At. Mol. Phys.* **18** 547–55
Mitchell J B A and McGowan J Wm 1978 *Astrophys. J.* **222** L77–9
Mul P M, McGowan J Wm, Defrance P and Mitchell J B A 1983 *J. Phys. B: At. Mol. Phys.* **16** 3099–107
Noren C, Yousif F B and Mitchell J B A 1989 *J. Chem. Soc. Faraday Trans. 2* **85** 1697–703
Prasad S S and Huntress W T 1980 *Astrophys. J. Supp.* **43** 1–35
Rakshit A B 1982 *Int. J. Mass Spectrom. Ion Phys.* **41** 185–97
Smith D and Adams N G 1980 *Top. Curr. Chem.* **89** 1–43
—— 1989 *J. Chem. Soc. Faraday Trans. 2* **85** 1613–30
Smith D, Adams N G, Dean A G and Church M J 1975 *J. Phys. D: Appl. Phys.* **8** 141–52
Turban G 1984 *Pure Appl. Chem.* **56** 215–30
Turner B E 1989 *Space Science Revs.* **51** 235–337
Vallée F B, Rowe B R, Gomet J C, Queffelec J L and Morlais M 1986 *Chem. Phys. Lett.* **124** 317–20
Weller C S and Biondi M A 1967 *Phys. Rev. Lett.* **19** 59–61
—— 1968 *Phys. Rev.* **172** 198–206
Yousif F B and Mitchell J B A 1989 *Phys. Rev.* A **40** 4318–21
Zipf E C 1980 *Geophys. Res. Lett.* **7** 645–8